Profile Extrusion and Mechanical Properties of Crosslinked Wood–Thermoplastic Composites

Magnus Bengtsson, Kristiina Oksman
Department of Engineering Design and Materials, Norwegian University of Science and Technology, 7491 Trondheim, Norway

Nicole M. Stark
Forest Products Laboratory, Forest Service, US Department of Agriculture, Wisconsin

Challenges for wood-thermoplastic composites to be utilized in structural applications are to lower product weight and to improve the long-term load performance. Silane crosslinking of the composites is one way to reduce the creep during long-term loading and to improve the mechanical properties. In this study, silane crosslinked wood-polyethylene composites were produced by reactive extrusion and subsequently manufactured into rectangular profiles. The silane crosslinked composites were stored in a sauna at 90 °C to increase the degree of crosslinking. The toughness of the silane crosslinked composites was significantly higher than for the non-crosslinked composites. Improved adhesion between the wood and polyethylene phases is most likely the reason for the improved toughness of the crosslinked composites. There was no significant difference in flexural modulus between the crosslinked and non-crosslinked composites. In addition, impact testing showed that the impact strength of the crosslinked composites was considerable higher (at least double) than the non-crosslinked. The effect of temperature on the impact strength of the composites indicated slightly higher impact strength at −30 °C than at 0° and at 25 °C, and then an incrase in impact strength at 60 °C. Crosslinking also reduced the creep response during short-term loading. Moreover, scanning electron microscopy on the fracture surface of the crosslinked composites revealed good adhesion between the polyethylene and wood phases. POLYM. COMPOS., 27:184–194, 2006. © 2006 Society of Plastics Engineers

INTRODUCTION

In recent years, the use of wood as reinforcing filler in plastics has received considerable attention. Wood provides advantages over conventional reinforcing materials such as low cost, abundancy, renewability, low specific gravity, and high specific strength and stiffness [1–3]. Wood–plastic composites are an alternative material for pressure treated wood. Pressure treatment of wood with chemical preservatives is necessary to retard biological decay and insect attack [4]. Chromated copper arsenate (CCA) is currently the most widely used wood preservative because of its excellent fungicidal and insecticidal properties [5]. However, the impact that CCA and other chemicals may have on the environment is a cause for concern. In addition, the treatments do little to resist the dimensional changes accompanying moisture absorption [4]. The plastic component in wood–plastic composites encapsulates the wood and thereby improves the durability against moisture and biological attack [6]. Moreover, wood plastic composites can be an alternative material for unfilled plastics. Wood–plastic composites can be readily processed in conventional processing equipment for plastics, such as extrusion and injection moulding. Addition of wood to the plastic matrix increases the stiffness of the material. When proper interfacial adhesion between the wood and the plastic matrix is achieved, the strength of the composite is also higher than for unfilled plastic.

In the last decade, there has been a lot of research in improving compatibility between the hydrophilic wood filler and the hydrophobic plastic matrix in wood–plastic composites. Stress transfer from the weaker plastic matrix to the stronger wood fibres plays an important role in determining the mechanical properties of the composites [7]. Many authors have published work on different types of coupling agents. One of the most commonly used coupling agents is maleic anhydride grafted polyolefins [7–11]. There have also been some studies on other types of coupling agents, such as silanes [12–14] and isocyanates [12–13]. A elastomeric copolymer, maleated styrene-(ethylene-*co*-butylene)-styrene (SEBS-*g*-MA), has also been reported to improve both the tensile strength and the impact strength of wood–plastic composites [15]. In our earlier studies, we

Correspondence to: Kristiina Oksman; e-mail: Kristina.oksman@ntnu.no
DOI 10.1002/pc.20177
Contract grant sponsor: Research Council of Norway.
Published online in Wiley InterScience (www.interscience.wiley.com).

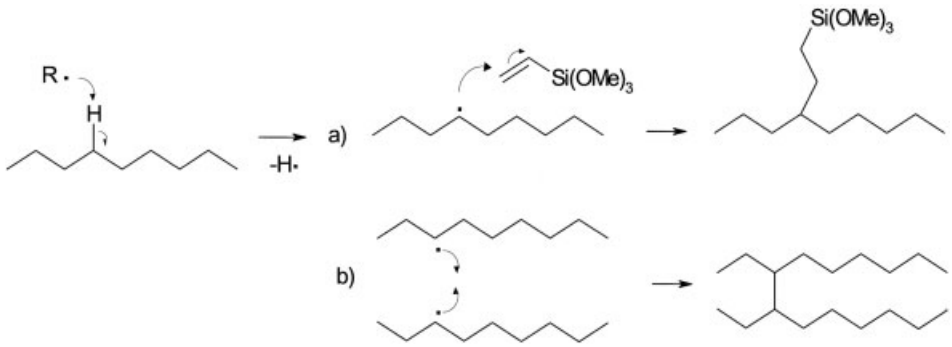

FIG. 1. The reaction mechanism during (a) peroxide induced melt grafting of vinyltrimethoxysilane on to polyethylene, (b) radical induced crosslinking of polyethylene.

have also shown that silane crosslinking improved the toughness and impact strength of wood–plastic composites through improved bonding at the wood–matrix interface [16–18].

According to Smith and Wolcott [4], challenges for wood–plastic composites for use in structural applications include develop structural design values, lower product weight, and improve long-term load performance. Existing wood–plastic composite products are typically used in applications where they are not critical structural elements [19]. For this reason, establishment of nominal design values for structural applications of these products has not been a high priority. As wood–plastic composite products extend to include more structural applications, it is necessary to determine appropriate structural design values. The density of wood–plastic composites is almost twice that of solid wood [20]. The weight of wood–plastic composites can be reduced by foaming of the wood–plastic composite [20–21]. Another way to reduce the weight of wood–plastic products is the use of hollow or shaped cross-sections [4]. Long-term material properties of wood–plastic composites also need improvements. Even though the durability of wood–plastic composites during outdoor exposure is superior to that of untreated wood, it is still a problem. Stark et al. [22] showed that wood–plastic composites experience a color change and loss in mechanical properties with accelerated weathering. Exposure to UV radiation and moisture during outdoor use is of particular concern for wood–plastic composites [22]. Furthermore, long-term load performance of wood–plastic composites also needs improvements. Wood–plastic composites experience a time-dependent behaviour when subjected to constant load. Creep is the increase in deformation over time when subjected to a sustained load [23]. Crosslinking of the polymer matrix is one way of reducing the creep during long-term loading of wood–plastic composites [16–18].

Several techniques have been developed to obtain crosslinked polyethylene: peroxide crosslinking, irradiation techniques, and silane crosslinking. However, both peroxide and irradiation crosslinking techniques involve high investment costs [24]. Other drawbacks are the risk of precuring and high production cost during peroxide crosslinking and the thickness limitation in radiation crosslinking [24]. The silane crosslinking technique does not suffer from high investment cost, and the ethylene-vinyl silane copolymer can be processed and shaped in conventional thermoplastic processing equipment and subsequently crosslinked after the processing steps. Grafting of vinyl silanes onto the polyethylene backbone is initiated by peroxide. The peroxide molecule dissociates by heat and forms radicals. The radicals have the potential to abstract hydrogen from the polyethylene polymer, but can also attack the vinyl group of the vinyltrimethoxy silane molecule and convert it into radicals. These free radicals either combine with one another or attack another molecule in the same fashion to propagate the free-radical reaction [25]. This process results in grafting of vinyltrimethoxy silane onto polyethylene; this is a prerequisite for crosslinking the material. Figure 1a shows the reaction mechanism during peroxide-induced melt grafting of vinyltrimethoxy silane onto polyethylene. The most prominent side reaction during melt grafting of vinyltrimethoxy silane onto high-density polyethylene is crosslinking or branching caused by radical–radical combination [26]. Figure 1b shows the reaction mechanism caused by radical induced crosslinking of polyethylene. Some of the crosslinked network in the specimens is thus caused by a radical–radical combination. The silane crosslinking reaction takes place in the presence of trace amounts of water. The silane crosslinking reaction proceeds over two steps as is shown in Figure 2. In the first step, the methoxyl groups are hydrolysed to hydroxyl groups when methanol is removed. The crosslinking takes place in the second step

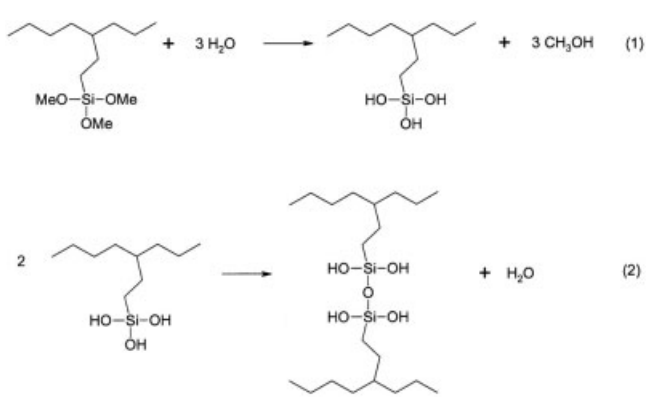

FIG. 2. The hydrolysis step (1) and condensation step (2) during silane crosslinking.

where the hydroxyl groups recombine through a condensation step [27].

Preparation of silane grafted composites can be performed in different ways. The plastic (or wood flour) can be treated with a diluted solution of vinyl silane/peroxide and the solvent subsequently evaporated before processing. Drawbacks of this method include the use of solvent and that the process is time consuming. Kuan et al. treated wood flour directly with vinyltrimethoxy silane without the use of solvent [28]. Another method is to pump the vinyl silane/peroxide solution directly into the extruder during processing. This can be done in a two-step process where the first step includes silane grafting of unfilled plastic and the second step incorporation of wood flour. This procedure was used in our first study of silane crosslinked composites [16]. In this study, the silane grafting and composite production were carried out simultaneously in a one-step process. By doing so, the production of composites is more economical and feasible on an industrial scale, and also gives the possibility of grafting silane onto both polyethylene and wood flour.

This study focused on processing silane crosslinked composites and evaluation of the mechanical properties of the composites. In the processing steps, silane crosslinked composites were produced and thereafter manufactured into rectangular profiles. The composites were cured at different humidities, to study how that affects the degree of crosslinking in the composites. Silane crosslinked composites with different degrees of crosslinking were then evaluated regarding their mechanical performance.

EXPERIMENTAL

Materials

High-density polyethylene, Exxon Mobile Chemicals HD6733 (*MFI* = 33 g/10 min, 190°C/2.16 kg), was obtained from Channel Prime Alliance (Norwalk, CT). Pine wood flour (40 mesh) was provided from American Wood Fiber (Schofield, WI). Vinyltrimethoxy silane (98%) and dicumyl peroxide (99%) were obtained from Sigma Aldrich (Leirdal, Norway). Lubricant, Struktol TMW113 was obtained from Struktol Company of America (Stow, OH). Throughout this article the crosslinked composites are, in figures and tables, referred to as "XLPE40" and the noncrosslinked as "HDPE40". Samples stored at room temperature and in a sauna are abbreviated RT and SA, respectively.

Compounding

The wood flour was dried for 24 h at 105°C, to a moisture content of ~0.9% (based on dry weight) before the compounding process. Plastic granulates and wood flour were compounded using a 32 mm Davis-Standard (Pawcatuck, CT) corotating twin-screw extruder with 7 temperature zones. The plastic (60% w/w) and the wood flour (40% w/w) were fed to the extruder at temperature zone 1 with Schenk AccuRate (Whitewater, WI) gravimetric feeders. Table 1, shows the processing parameters during compounding. The zone temperatures ranged 171–193°C, the screw speed was 200 rpm, the melt pressure at the die varied between 15 and 39 bar depending on material blend, and the material output was 6.8 kg/h. Silane crosslinked composites were produced by pumping a solution of vinyltrimethoxy silane and dicumyl peroxide (12:1 w/w) into the extruder at temperature zone 1. The amount of added silane solution to the composites was 2% w/w. Vacuum venting at temperature zone 8 was used to minimize volatile extractives and unreacted silane in the final samples. The extruded composite strands were cooled with compressed air and granulated with the use of a Primo 120E (Rieter, Spartanburg, SC) pelletizer.

TABLE 1. Processing settings during compounding.

	Noncrosslinked (HDPE40)	Crosslinked (XLPE40)
Overall rate (kg/h)	6.82	6.82
Plastic feeder (kg/h)	4.09	3.95
Wood feeder (kg/h)	2.73	2.73
Silane solution (kg/h)[a]	–	0.14
Feed section (°C)	20	20
Zone 1 (°C)	193	193
Zone 2 (°C)	188	188
Zone 3 (°C)	174	174
Zone 4 (°C)	174	174
Zone 5 (°C)	174	174
Zone 6 (°C)	171	171
Zone 7 (°C)	171	171
Die	174	174
Vent pressure zone 8	Vaccum	Vaccum
Screw speed (rpm)	200	200
Melt temperature (°C)	186	188
% Load	29	43
Melt pressure (bar)	15	39

[a] A solution of vinyltrimethoxy silane and dicumylperoxide (12:1).

Profiling

The compounded composite granulates were dried for 24 h at 105°C, to a moisture content of ~0.3% (based on dry weight) before the profiling. Profiles were produced in the same corotating extruder through a rectangular die measuring 6.4×60 mm^2. The composite granulates (96% w/w) and lubricant (4% w/w) was gravimetrically fed to the extruder at temperature zone 1. As is shown in Tables 2 and 3, the processing settings varied depending on material formulation. The temperatures ranged 191–116°C, the screw speed ranged 150–30 rpm, the melt pressure at the die varied between 0 and 17 bar, and the material output was 6.8 kg/h. A water spray tank was used to cool the extruded profiles and a puller pulled the profiles through the water spray tank. Standard test specimens for mechanical testing

DOI 10.1002/pc

TABLE 2. Processing setting during profiling of noncrosslinked composites (HDPE40).

Formulation	1	2	3	4	5[a]
Overall rate (kg/h)	6.82	6.82	6.82	6.82	6.82
Composite feeder (kg/h)	6.82	6.82	6.82	6.55	6.55
Lubricant feeder (kg/h)	–	–	–	0.27	0.27
Feed section (°C)	20	20	20	20	20
Zone 1 (°C)	188	166	166	182	182
Zone 2 (°C)	188	160	160	182	182
Zone 3 (°C)	188	160	160	177	177
Zone 4 (°C)	188	154	154	143	143
Zone 5 (°C)	188	149	149	127	127
Zone 6 (°C)	188	149	149	121	118
Zone 7 (°C)	182	149	149	121	116
Die	177	143	143	132	132
Die 2	160	143	143	135	135
Vent pressure zone 8	Vaccum	Vaccum	Vaccum	Vaccum	Vaccum
Screw speed (rpm)	150	150	40	30	30
Melt temperature (°C)	183	150	145	129	129
% Load	28	31	85	50	48
Melt pressure (bar)	0	0	0	6	14

[a] The composite formulation used for testing.

were cut from the profiles. Part of the samples was stored at room temperature and the others were stored for 48 h in a simulated sauna. The storage conditions in the sauna were approximately 100% RH and 90°C. The sauna stored samples were subsequently dried to their initial weight before testing.

Melt Flow Index

Melt flow index (MFI) measurements of composite granulates were obtained using a Galaxy I Melt Indexer, Model 750 (Kayeness, Morgantown, PA). The measurements were performed at 190°C with a 2.16 kg load, in accordance with ASTM D1238 standard.

TABLE 3. Processing setting during profiling of crosslinked composites (XLPE40).

Formulation	1	2	3	4[a]
Overall rate (kg/h)	6.82	6.82	6.82	6.82
Composite feeder (kg/h)	6.55	6.55	6.55	6.55
Lubricant feeder (kg/h)	0.27	0.27	0.27	0.27
Feed section (°C)	20	20	20	20
Zone 1 (°C)	188	188	188	188
Zone 2 (°C)	188	188	188	188
Zone 3 (°C)	188	188	177	177
Zone 4 (°C)	188	188	166	154
Zone 5 (°C)	188	188	154	149
Zone 6 (°C)	177	177	149	143
Zone 7 (°C)	177	177	149	143
Die	182	182	177	177
Die 2	191	191	179	179
Vent pressure zone 8	Vacuum	Vacuum	Vacuum	Vacuum
Screw speed (rpm)	100	50	50	30
Melt temperature (°C)	184	183	171	168
% Load	27	30	34	47
Melt pressure (bar)	16	17	12	13

[a] The composite formulation used for testing.

Gel Content

The gel content of the samples was determined using *p*-xylene extraction, according to ASTM D2765. The specimens to be analyzed were ground and placed in folded 120 mesh stainless steel cloth cages. Cages with ground samples were weighed before immersion in the *p*-xylene. Butylated hydroxytoluene (BHT) was used as an antioxidant to inhibit further crosslinking of the specimen, and 1% of BHT was dissolved in the *p*-xylene. The cages with ground material were then extracted in boiling *p*-xylene/BHT solution (143°C) for 12 h. Extracted specimens were then dried at 150°C until a constant weight was attained and subsequently reweighed. The gel content of the different blends was determined as the average of two separate analyses. The gel-content was calculated according to the following equation:

$$\text{Extract \%} = (\text{weight lost during extraction})/(\text{weight of original specimen-weight of filler})$$

$$\text{Gel content} = 100 - \text{Extract \%}. \quad (1)$$

Mechanical Testing

Flexural properties of the samples were measured on a Tinius Olsen H5K-S UTM equipment (Horsham, PA), in accordance with ASTM D790. The dimensions of the specimens tested were approximately $3.2 \times 12.7 \times 130$ mm^3. The measurements were performed at ambient conditions, i.e. a temperature of 23°C and a relative humidity of approximately 50%. At least 10 specimens of each blend were tested.

Instrumented drop weight impact tests were performed on a Dynatup GRC 8250 impact tester (Instron, Norwood, MA) at a speed of 1 m/s. The dimensions of the unnotched composite specimens tested were approximately $3.2 \times 12.7 \times 130$ mm^3. The composites were impacted in bending mode, and were not clamped down. A GRC EC 8250 environmental chamber was used to conduct impact tests at −30, 0, 25, and 60°C. The specimens to be analyzed were kept for at least 30 min at the chosen temperature before performing the test. All data were analyzed using instron dynatup impulse data acquisition system (Version 2.2.0, Instron, Norwood, MA) At least 10 specimens of each blend were tested at the four different temperatures.

Short-term creep experiments of composites were performed using a rheometrics dynamic mechanical thermal analyzer DMTA V (Rheometric Scientific, Piscataway, NJ). The measurements were performed in dual cantilever mode on specimens measuring approximately $2 \times 12 \times 30$ mm^3.

The creep response of the composites was measured when subjected to an applied static stress of 3 MPa for 3 days and subsequently 3 days of recovery. All experiments were performed at a temperature of 30°C.

Scanning Electron Microscopy

Scanning electron microscopy (SEM) was used to monitor the fracture surface of the composites after quenching the composites in liquid nitrogen. SEM analysis was performed using a Hitachi S-4300 field emission SEM (Hitachi Science Systems Japan) at an accelerating voltage of 15 kV. The composites were sputtered with a layer of gold/palladium before the measurements.

RESULTS AND DISCUSSION

Processing

In the compounding step, grafting of vinyltrimethoxy silane onto polyethylene and wood flour and composite production was carried out simultaneously in a one-step process. A ratio of approximately 5:1 between residence time in the extruder (at the actual temperatures) and the half life time of the peroxide was used. If the residence time corresponds to five-half lives there will be $>$ 97% consumption of the peroxide [26]. As can be seen in Table 1, addition of a solution of vinyltrimethoxy silane and dicumyl peroxide during compounding increased the motor load and melt pressure in the extruder. An increase in melt viscosity of polyethylene upon silane grafting was expected. This increase in melt viscosity is due to premature crosslinking but the melt viscosity will also increase as a result of interaction between grafted silane groups [26]. A higher melt viscosity and the volatile compounds created during melt grafting reactions contribute to the increased melt pressure. In our previous study, we showed that an addition of 4% or more of silane solution during the grafting process was necessary to be able to fully crosslink the material at 90°C, at near saturation within 48 h [18]. The addition of silane solution in this study was limited to 2% w/w, since at higher level of silane solution addition the melt pressure limit of the extruder was reached.

The compounded granulates were manufactured into rectangular profiles (6.4 $\times$ 60 mm^2). According to the supplier, the MFI of the high-density polyethylene used was 33. After addition of wood flour to the polyethylene, the MFI of the noncrosslinked granulates was still rather high and measured to 4.8. The relatively low melt viscosity of the noncrosslinked composite melt made it difficult to handle downstream through the water spray tank, without creating an irregular structure. As can be seen in Table 2, the approach to minimize the irregular structure was to lower the melt temperature by a stepwise decrease in screw speed and heating temperature in the last part of the extruder. A decrease in melt temperature increases the motor load. The use of lubricant and the relatively high heating temperature in the beginning of the extruder made it possible to keep the motor loading down while the melt temperature was decreased. In this way, the surface smoothness and appearance of the noncrosslinked composite profiles was improved. However, it was not possible to achieve a completely smooth surface structure of the noncrosslinked profiles (see Fig. 3). The melt viscosity of the crosslinked composites was much higher than for the noncrosslinked composites as a result of premature crosslinking and interaction between grafted silane groups. It was not possible to measure the MFI of the crosslinked granulates, since the melt viscosity was too high. However, the shear forces introduced during extrusion made it possible to profile the crosslinked composite. The higher melt viscosity of the crosslinked composite made it easier to handle downstream through the water spray tank without creating an irregular structure. As is shown in Table 3, the melt temperature was lowered stepwise during profiling of the crosslinked composites until a regular structure was achieved. In our previous study [18], we found that edge-tearing and rough surface of the final crosslinked composites were a problem. In that study, no lubricant was used because of the risk of interference with the silane solution during the grafting process. Also in this study, edge-tearing and a rough surface of the crosslinked profiles was a problem when no lubricant was used. These problems are believed to be caused by encapsulating problems of the wood flour. However, the use of 4% w/w of lubricant removed the rough surface and the edge-tearing of the crosslinked profiles (see Fig. 3). Possible interference between lubricant (modified fatty esters) and silane is not believed to be as critical during the profiling step (second step), as it would be during the grafting step.

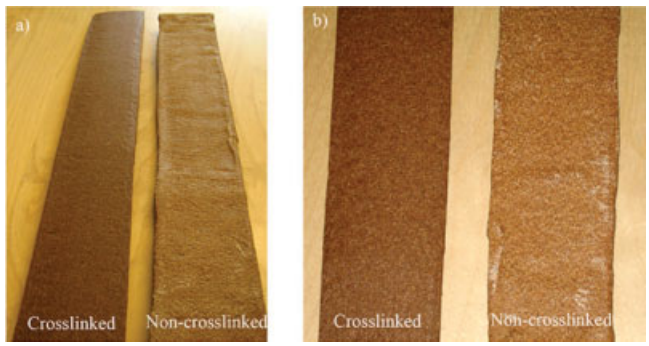

FIG. 3. (a) The final appearance of the crosslinked and noncrosslinked siding profiles. (b) Magnification of the profiles in figure (a). [Color figure can be viewed in the online issue, which is available at www.interscience.wiley.com.]

Degree of Crosslinking

The degree of crosslinking in the composites was determined by gel content measurements. The gel content was determined in accordance with ASTM D2765. Crosslinked polyethylene is insoluble in boiling *p*-xylene whereas the

DOI 10.1002/pc

TABLE 4. Gel content of the composites.

Sample code	Gel content (%)
HDPE40-RT	0
XLPE40-RT	33
XLPE40-SA	59

noncrosslinked part is soluble. The gel content can thus be determined gravimetrically from the extracted samples. The first step in the crosslinking reaction is hydrolysis of the methoxyl groups to silanol groups. Water is responsible for the hydrolysis of the methoxyl groups. A higher humidity level in the curing process would thus be expected to create a higher degree of crosslinking in the samples. As can be seen in Table 4, storage in a high humidity sauna generated a higher degree of crosslinking (59%) in the composites than storage at room temperature (33%). In a previous study, it was shown that storage of silane-modified composites at room temperature did not significantly affect the gel content in the composites [17]. The degree of crosslinking in the composites stored at room temperature is thus believed to correspond to the crosslinking that takes place during processing. Earlier studies have shown that the maximum gel content during silane crosslinking is in the range 75–80% [17, 27]. It was shown that an addition of 4% w/w or more of the silane solution during processing was necessary to fully crosslink the composites cured at 90°C at near saturation, when no catalyst was used. The addition of silane solution in this study was limited to 2% w/w, since at higher level of silane solution addition, the melt pressure limit of the extruder was reached. The rate of the crosslinking reaction can be increased by incorporation of a tin-based catalyst (dibutyl-tin-dilaurate, DBTDL) during processing [27]. Incorporation of such catalyst would increase the rate of crosslinking of the plastic but could on the other hand counteract the reaction with wood. DBTDL has been shown to increase the rate of both the reaction steps in the crosslinking, i.e. hydrolysis and condensation [27]. In the presence of DBTDL, formation of an ether bond between plastic and wood (—Si—O—Wood) could be catalyst back to a silanol group. The use of catalyst would also make the final composite product more expensive.

Mechanical Properties

The flexural properties of the composites were determined in accordance with ASTM D790. Figure 4 shows characteristic stress–strain curves of the composites. The crosslinked composites showed flexural strength superior to the composites to which no silane was added. In our previous study, silane crosslinked composites also showed flexural strength superior to the noncrosslinked composites [18]. In that study, the flexural strength was shown to pass through a maximum range 2–3% w/w of added silane solution and then decreased slowly. Improved adhesion between the wood and the polyethylene matrix is most likely

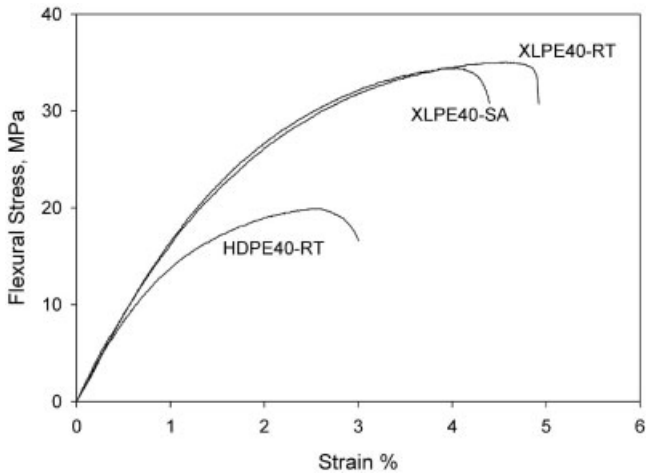

FIG. 4. Characteristic stress–strain curves of the composites.

the reason for the significant improvement in flexural strength of the crosslinked composites. The improved adhesion could be due to covalent bonding between wood and polyethylene through either condensation or free-radical reaction. Moreover, hydrogen bonding between silanol groups grafted on polyethylene and hydroxyl groups on wood, as well as van-der-Waals forces between condensated silane on wood and the polyethylene matrix, can improve the adhesion between the phases (see Fig. 5). Curing the crosslinked composites in a high humidity sauna increased the degree of crosslinking in the composites significantly (i.e. 33–59%). Even so, the flexural strength of the composites cured in a sauna did not differ much from the crosslinked composites stored at room temperature. This

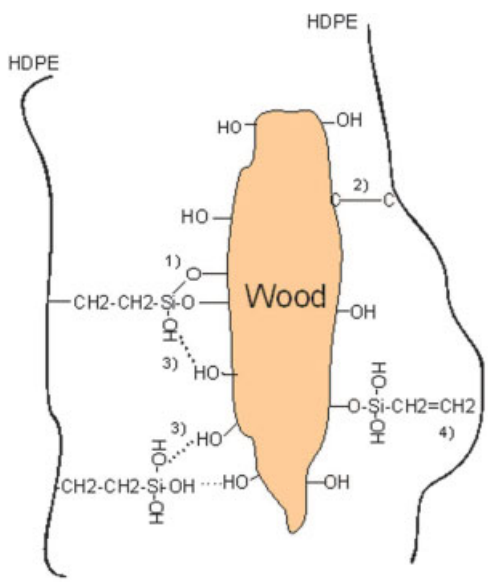

FIG. 5. Proposed bonding mechanisms in the silane crosslinked composites. Covalent bonding between wood and polyethylene through condensation (1) and free-radical reaction (2). Secondary interactions through hydrogen bonding (3) and van der Waals interaction (4). [Color figure can be viewed in the online issue, which is available at www.interscience.wiley.com.]

TABLE 5. Flexural properties of the composites.

Sample code	Modulus (GPa)	Strength (MPa)	Strain at max (%)
HDPE40-RT	1.6 ± 0.2	19.4 ± 2.3	2.8 ± 0.7
XLPE40-RT	1.9 ± 0.3	36.2 ± 3.0	4.5 ± 0.2
XLPE40-SA	1.9 ± 0.2	33.9 ± 2.2	3.9 ± 0.2

indicates that the reactions responsible for improving the adhesion between wood and polyethylene mainly takes place during the higher temperature used during processing. All the mechanical data from the flexural testing are summarised in Table 5. The elongation at break was also higher in the crosslinked composites than for the noncrosslinked. Improved adhesion between wood and polyethylene in the crosslinked composites is believed to explain the improved toughness. Without interfacial adhesion, the gap between the wood and polyethylene phases provides an area of weakness, which easily propagates a crack through the material.

There was no significant difference in flexural modulus between the crosslinked and noncrosslinked composites. However, the crosslinked composites seem to have a slightly higher flexural modulus than the noncrosslinked composites. In our previous study, the flexural modulus of silane crosslinked composites was shown to be lower than for the noncrosslinked, and was also shown to decrease at increased level of added silane solution. The decrease in flexural modulus was shown to correlate well with the crystallinity of the polyethylene matrix in the composites. At higher level of silane addition, the premature crosslinking during processing increased and thereby lowered the degree of crystallinity as a result of restriction in macromolecular flexibility in the melt. In this study, the addition of silane solution was rather low (2% w/w) and the premature crosslinking that took place during processing was also shown to be low (33%). The rather low degree of premature crosslinking during processing is believed to explain why no decrease in flexural modulus was observed. The increased crosslinking that occurs during curing in a sauna occurs when the composite is in the solid state. Therefore, the crystalline phase of the HDPE should not undergo considerable changes and the crosslinking preliminary should take place only in the amorphous phase. This explains why there is no significant change in flexural modulus between the crosslinked composites stored in a sauna and at room temperature.

Instrumented drop weight impact tests on un-notched composite specimens were carried out. The test was performed to study the effect of temperature on the impact properties of crosslinked and noncrosslinked composites. Figure 6 illustrates characteristic force-deflection curves from impact testing of the composites stored at room temperature. As can be seen in the figure, the crosslinked and the noncrosslinked composites show relatively linear loading curves, ending in a rather sharp drop after reaching

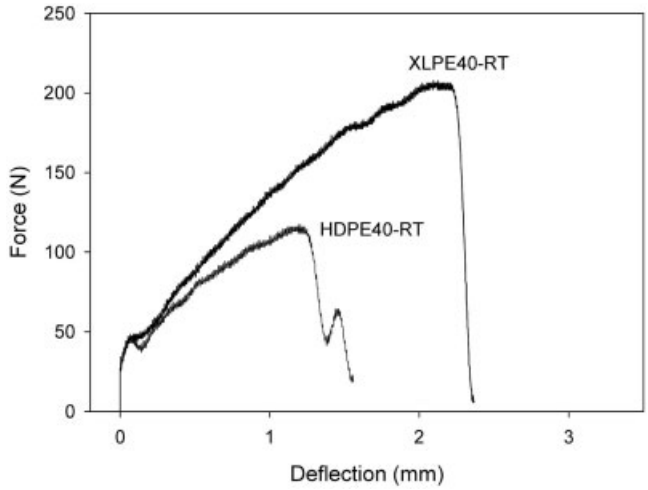

FIG. 6. Characteristic force-deflection curves from impact testing of the composites stored at room temperature.

maximum load. The maximum load and deflection at failure was significantly higher for the crosslinked than for the noncrosslinked composites. This reveals a higher impact resistance in the crosslinked composites than in the noncrosslinked. The effect of temperature on the impact strength of the composites is presented in Figure 7 and Table 6. Independent of temperature, the impact strength was significantly higher (about two times) in the crosslinked composites than in the noncrosslinked. Improved adhesion between wood and polyethylene and improved impact strength of the polyethylene matrix upon crosslinking, can explain the superior impact strength of the crosslinked composites. In the temperature range −30 to 60°C, it is difficult to make certain statements about trends in impact strength among the crosslinked and noncrosslinked composites because the standard deviation within the two groups is overlapping. The trend, however, seems to be a slightly higher impact strength at −30°C than at 0°C and 25°C, and then an

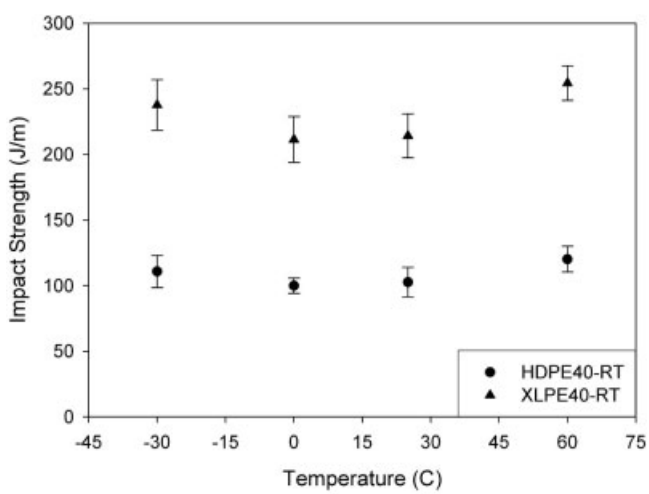

FIG. 7. The effect of temperature on the impact strength of the composites.

DOI 10.1002/pc

TABLE 6. Impact strength (J/m) of the composites at different temperatures.

	Temperature (°C)			
Sample code	−30	0	25	60
HDPE40-RT	111 ± 12	100 ± 12	102 ± 11	120 ± 10
XLPE40-RT	238 ± 19	211 ± 26	214 ± 17	254 ± 13

increase in impact strength at 60°C. High-density polyethylene has two major transitions when heat treated, corresponding to γ-transition occurring at about −128°C and then the α-transition at about 113°C [29]. Unplasticized HDPE does not display an apparent β-transition because its crystallinity greatly reduces the relaxation intensity [29]. The impact strength of the composites was thus determined in a temperature range in between the two major temperature transitions of high-density polyethylene. This might explain why the impact strength did not differ significantly in the temperature range −30 to 60°C within the two composite blends. It is interesting to note that the increase in impact strength at 60°C was more significant for the crosslinked composite than for the noncrosslinked. Crosslinked polyethylene was introduced in market to improve the temperature durability of polyethylene [27]. One could thus expect the crosslinked composite to perform better at higher temperature than the noncrosslinked composite.

Short-term creep experiments were performed using a dynamic mechanical thermal analyzer, DMTA V. The experiments were performed to study the effect of silane crosslinking on the creep properties of the composites. In Figure 8, the results from the short-term creep test of noncrosslinked and crosslinked (stored in a sauna) composites are shown. The creep response after 3 days of loading was significantly lower in the crosslinked composites than in the noncrosslinked composite. It is interesting to note that the creep rate (mm/day) during loading is more than twice as fast for the noncrosslinked composite than for the crosslinked. After 3 days of recovery, the nonrecoverable deformation was also larger in the noncrosslinked composite (0.66%) than in the crosslinked (0.23%). The improved creep properties of the crosslinked composites are believed to be related to a reduced viscous flow of the polyethylene matrix because of crosslinking as well as improved adhesion between the polyethylene matrix and wood flour. In an earlier study of silane crosslinked composites, it was also shown that a higher degree of crosslinking lowered the creep response [17]. In that study, crosslinked composites stored in a sauna showed lower creep response than composites stored at room temperature.

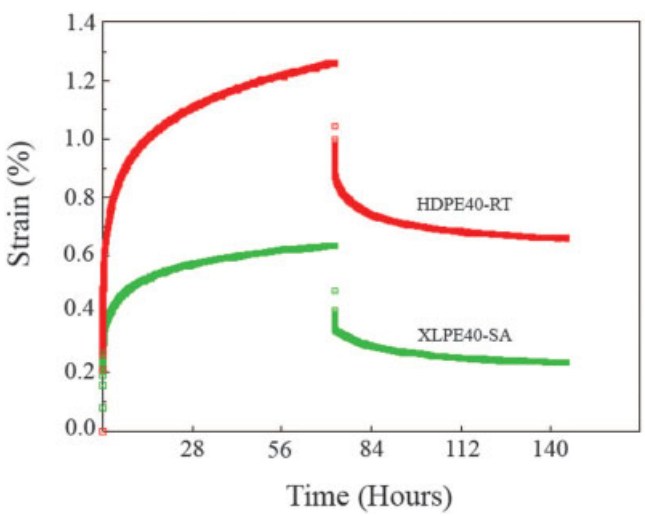

FIG. 8. Strain as a function of time during creep experiments at 30°C. A constant stress of 3MPa was applied during the loading time. [Color figure can be viewed in the online issue, which is available at www.interscience.wiley.com.]

Scanning Electron Microsscopy

SEM was used to monitor the fracture surface of the composites after quenching the samples in liquid nitrogen. In Figures 9 and 10, the fracture surfaces of noncrosslinked and crosslinked composites are shown. A comparison of the overview micrographs of the noncrosslinked (Figs. 9a and 9d) and the crosslinked (Figs. 10a and 10d) composite shows that it is much easier to visualize the wood filler in the noncrosslinked composite than in the crosslinked where the wood filler to a greater extent is covered with matrix. The fracture surface of the noncrosslinked composite shows several holes and patterns from wood fibres, which were so weakly bonded to the matrix that they were released from the matrix during fracture. In the upper right corner and on the left side of micrograph 9a examples of such holes and patterns from released wood fibres are shown. In the magnified micrographs 9c and 9f, it is also possible to notice distinct gaps between the matrix and the wood fibres, indicating poor adhesion. In the crosslinked composite (sauna stored), on the other hand, there is no gap between the matrix and the wood fibre, indicating good interfacial adhesion. This is visualized in the magnified micrographs 10c and 10f. In micrograph 10f, it is also possible to picture wood fibres covered with a thin layer of polyethylene matrix. In addition, the crosslinked composites show almost no signs of fibre pull-outs and most of the fibres fractured.

CONCLUSIONS

Silane crosslinked composites were produced during compounding in a co-rotating twin-screw extruder. Addition of silane solution during compounding increased the melt viscosity significantly, as a result of both premature crosslinking and interaction between grafted silane groups. Composite granulates were subsequently extruded into rectangular profiles. The higher melt viscosity of the crosslinked composite than the non-

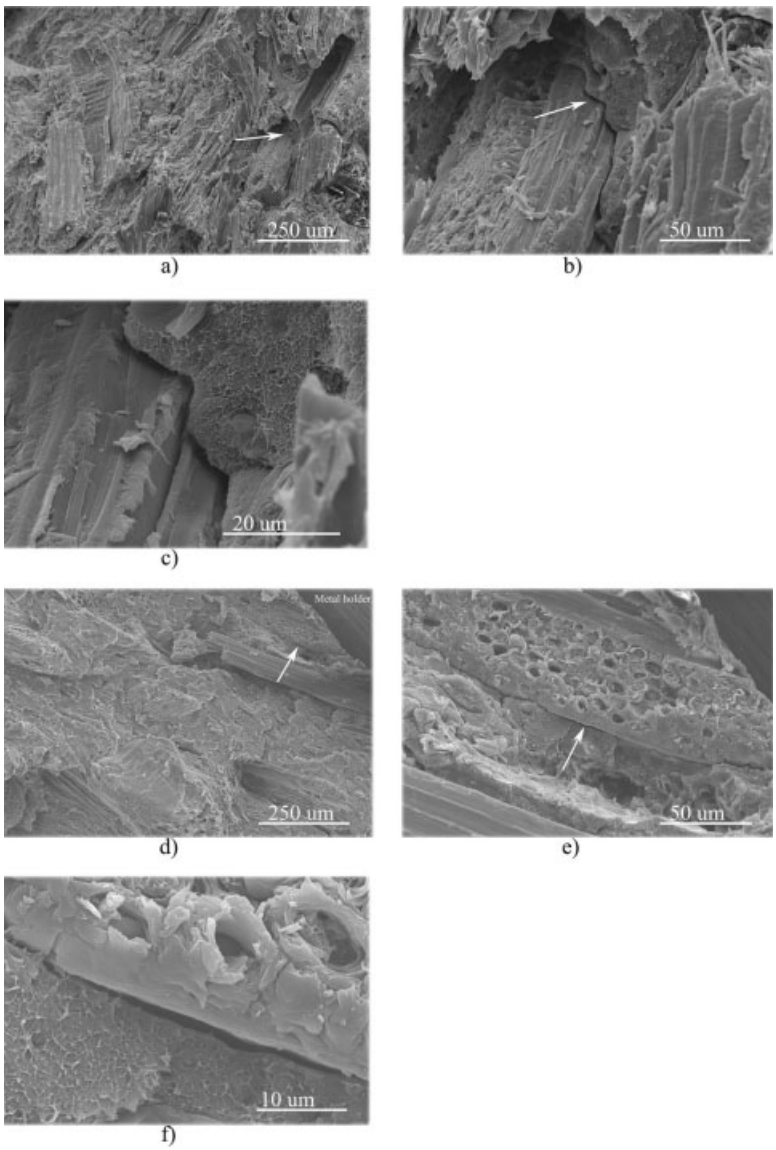

FIG. 9. SEM analysis of the fracture surface of the noncrosslinked composite at (a) ×120 (b) ×600 (c) ×2000 (d) ×120 (e) ×600 (f) ×3000.

crosslinked made it easier to handle downstream without creating an irregular structure. On the other hand, edge-tearing and a rougher surface on the crosslinked composites were a problem during profiling. Addition of lubricant removed the rough surface and the edge-tearing on the crosslinked profiles. The crosslinking reaction was shown to be initiated already during the processing steps. Storage in a high humidity sauna at 90°C generated a higher degree of crosslinking in the composites than storage at room temperature.

The flexural strength and elongation at break was significantly higher in the silane crosslinked composites than in the noncrosslinked. The improved toughness in the crosslinked composites is most likely caused by improved adhesion between the wood and polyethylene phases. There was no significant difference in flexural modulus between the crosslinked and noncrosslinked composites, although the crosslinked composites seem to have a slightly higher modulus. Impact testing showed that the impact strength of the crosslinked composites was considerably higher (at least double) than the noncrosslinked. This was explained as a result of both improved adhesion between wood and polyethylene and improved impact strength of the polyethylene matrix upon crosslinking. In the temperature range −30 to 60°C, the trend in impact strength among the crosslinked and noncrosslinked composites indicated slightly higher impact strength at −30°C than at 0°C and 25°C, and then an increase in impact strength at 60°C. The increase in impact strength at 60°C was also more significant for the crosslinked composites than for the noncrosslinked. Moreover, short-term creep analysis showed that the creep response during loading in the crosslinked composites was significantly lower than in the noncrosslinked. After recovery, the unrecoverable part was also larger in the noncrosslinked composite than in the crosslinked. The improved creep properties of the crosslinked composites was related to a reduced viscous flow due to crosslinking, as well as to improved adhesion between the polyethylene matrix and wood flour.

 DOI 10.1002/pc

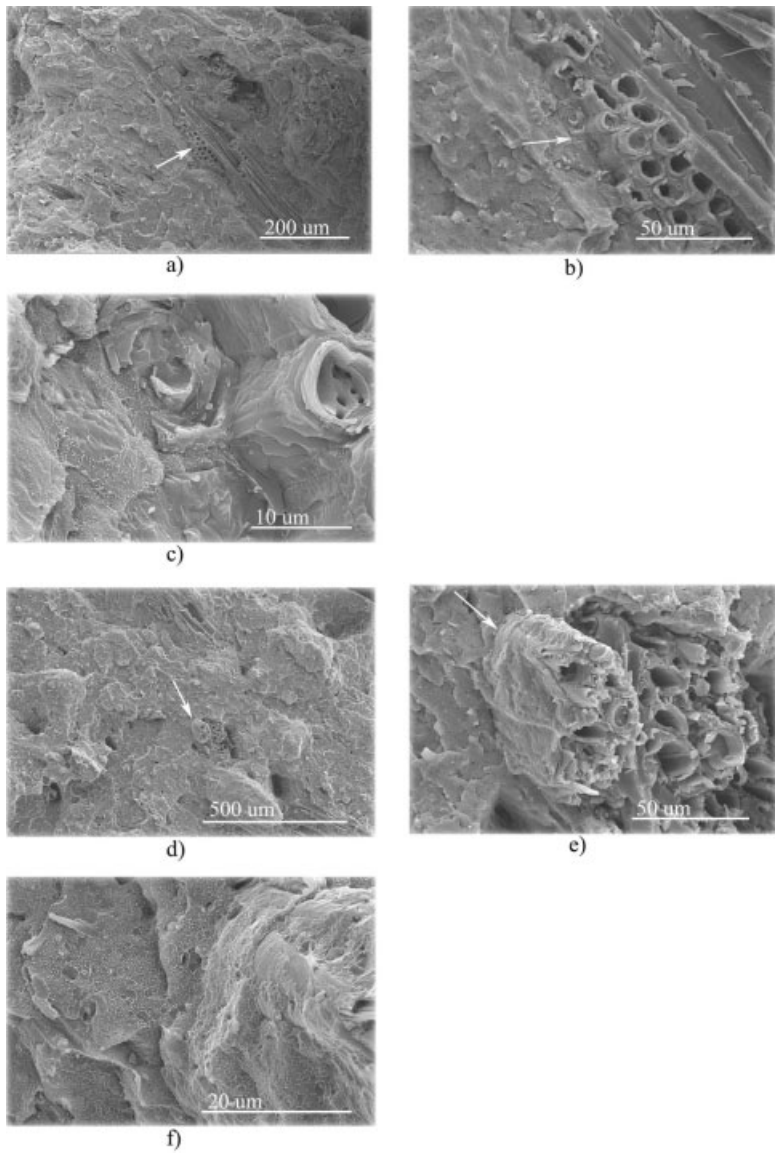

FIG. 10. SEM analysis of the fracture surface of the crosslinked composite at (a) ×150 (b) ×800 (c) ×3500 (d) ×100 (e) ×800 (f) ×2500.

SEM analysis on the fracture surface of the non-crosslinked composite showed holes in the matrix from pulled out fibres. In addition, there were distinct gaps between the polyethylene and the wood, indicating poor interfacial adhesion. The crosslinked composites, on the other hand, showed no gap between the polyethylene and the wood, indicating good interfacial adhesion. Moreover, the crosslinked composites showed almost no signs of fibre pull-outs and most of the fibres fractured.

ACKNOWLEDGMENTS

The authors thank Neil Gribbins and David Marr for their help with the processing of the composites. The authors also gratefully acknowledge American Wood Fibers (Schofield, WI, US) for supplying the wood flour.

REFERENCES

1. A.K. Bledzki, S. Reihmane, and J.J. Gassan, *Polym. Plast. Technol. Eng.*, **37**, 451 (1998).
2. H. Dalaväg, C. Klason, and H.E. Strömvall, *Int. J. Polym. Mater.*, **11**, 9 (1985).
3. P. Zadorecki and A.J. Michell, *Polym. Compos.*, **10**, 69 (1989).
4. M.P. Wolcott and M.S. Smith, *Proceedings of Progress in Woodfibre-Plastic Composites Conference 8th (Toronto)*, **1**, 1 (2004).
5. D. Stilwell, M. Toner, and B. Sawhney, *Sci. Total. Environ.*, **312**, 123 (2003).
6. D.P. Harper and M.P. Wolcott, *Composites Part A.*, **35**, 385 (2003).
7. S.M. Lai, F.C. Yeh, Y. Wang, H.C. Chan, and H.F. Shen, *J. Appl. Polym. Sci.*, **87**, 487 (2003).
8. D. Maldas and B.V. Kokta, *Int. J. Polym. Mater.*, **27**, 77 (1994).

9. J. Felix and P. Gatenholm, *J. Appl. Polym. Sci.*, **42**, 609 (1991).
10. M. Kazayawoko, J.J. Balatinecz, and L.M. Matuana, *J. Mater. Sci.*, **34**, 6189 (1999).
11. K. Oksman and C. Clemons, *J. Appl. Polym. Sci.*, **67**, 1503 (1998).
12. B.V. Kokta, R.G. Raj, and C. Daneault, *Polym. Plast. Technol. Eng.*, **28**, 247 (1989).
13. R.G. Raj, B.V. Kokta, D. Maldas, and C. Daneault, *J. Appl. Polym. Sci.*, **7**, 1089 (1989).
14. H.C. Kuan, J.M. Huang, C.C.M. Ma, and F.Y. Wang, *Plast. Rubber. Compos.*, **2**, 122 (2003).
15. K. Oksman, *Wood. Sci. Tech.*, **30**, 196 (1996).
16. M. Bengtsson, P. Gatenholm, and K. Oksman, *Compos. Sci. Technol.*, **65**, 1468 (2005).
17. M. Bengtsson and K. Oksman, *Composites Part A.,* (in press).
18. M. Bengtsson and K. Oksman, *Compos. Sci. Technol.*, (in press).
19. S.A. Davidow and K.J. Fridley, *J. Mater. Civ. Eng.*, **15**, 415 (2003).
20. Q. Li and L.M. Matuana, *J. Appl. Polym. Sci.*, **88**, 3139 (2003).
21. L.M. Matuana, C.B. Park, and J.J. Balatinecz, *Polym. Eng. Sci.*, **38**, 1862 (1998).
22. N.M. Stark and L.M. Matuana, *J. Appl. Polym. Sci.*, **94**, 2263 (2004).
23. I.M. Ward and D.W. Hadley, *An Introduction to the Mechanical Properties of Solid Polymers,* Wiley, Chichester (1993).
24. N.C. Liu, G.P. Yao, and H. Huang, *Polymer*, **41**, 4537 (2000).
25. G.B. Shah, M. Fuzail, and J.J. Anwar, *J. Appl. Polym. Sci.*, **92**, 3796 (2004).
26. G. Moad, *Prog. Polym. Sci.*, **24**, 81 (1999).
27. T. Hjertberg, M. Palmlöf, and B-Å. Sultan, *J. Appl. Polym. Sci.*, **42**, 1185 (1991).
28. C.F. Kuan, H.C. Kuan, C.C.M. Ma, C.C. Lin, and Y.K. Hsiao, *Annual Technical Conference—Society of Plastics Engineers 62nd (Chicago)*, **3**, 2947 (2004).
29. R.P. Chartoff, "Thermoplastic Polymers", in *Thermal Characterization of Polymeric Materials, Vol. 2,* Academic Press, San Diego (1996).

 DOI 10.1002/pc